Evaporitos

Sedimentologia – GSA0252

Prof. Dr. André Marconato

Introdução

- Evaporitos?

Introdução

- Evaporitos?
  - Depósitos formados por minerais precipitados por evaporação a partir de soluções saturadas

Introdução

- Evaporitos?
  - Depósitos formados por minerais precipitados por evaporação a partir de soluções saturadas
  - Volume muito menor que depósitos carbonáticos (embora possam ser espessos)
  - Formados principalmente por halita, gipso e anidrita

Classificação

- Habitualmente classificados entre evaporitos marinhos e não-marinhos
- Podem ser classificados de acordo com a composição (ânion)

Classificação

Major types	Subtypes	Composition and nature	
Marine evaporites (subaqueous and subaerial–sabkha precipitation)			
Chlorides	Halite	$NaCl$	Rock salt
	Sylvite	KCl	
	Carnallite	$KMgCl_3.6H_2O$	
Sulphates	Langbeinite	$K_2Mg_2(SO_4)_3$	Potash salts or bitterns
	Polyhalite	$K_2Ca_2Mg(SO_4)_4.2H_2O$	
	Kainite	$KMg(SO_4)Cl.3H_2O$	
	Anhydrite	$CaSO_4$	
	Gypsum	$CaSO_4\ 2H_2O$	
	Kieserite	$MgSO_4.H_2O$	
Carbonates	Calcite	$CaCO_3$	Inorganic carbonates
	Magnesite	$MgCO_3$	
	Dolomite	$CaMg(CO_3)_2$	

Stow (2005)

Classificação

Non-marine evaporites		
Chlorides	Halite	NaCl
	Rinneite	$FeCl_2.NaCl.3KCl$
Sulphates	Gypsum	$CaSO_4 2H_2O$
	Anhydrite	$CaSO_4$
	Epsomite	$MgSO_4.7H2O$
	Mirabilite	$Na_2SO_4.10H_2O$
	Thenardite	Na_2SO_4
	Bloedite	$Na_2SO_4.MgSO_4.4H_2O$
	Glauberite	$CaSO_4.Na_2SO_4$
Carbonates	Natronite	$Na_2CO_3.10H_2O$
	Trona	$NaHCO_3.Na_2CO_3.2H_2O$
	Gaylussite	$Na_2CO_3.CaCO_3.5H_2O$
Borates	Borax	$Na_2B_4O_5(OH)_4 8H_2O$
Silicates	Magadiite	$NaSi_7\ O_{13}(OH)_3.3H_2O$

Stow (2005)

Tipos de evaporito

- Gipso e anidrita
  - Deposição como gipso (hidratado)
    - Alterado para anidrita ou pseudomorfos de anidrita ainda no ambiente deposicional
    - Poucos metros de soterramento alteram gipso para anidrita por perda de água → perda de até 38% do vol.

Tipos de evaporito

- Gipso e anidrita
  - Seguidas mudanças de volume distorcem a fábrica (estrutura e textura) sedimentar de gipso
  - Três grupos de estruturas de anidrita:
    - Anidrita nodular
    - Anidrita laminada
    - Anidrita maciça

Tipos de evaporito

- Estrutura *tepee*

Richi Lucchi (1996)

Tipos de evaporito

- Anidrita nodular
  - Formada por deslocamento por crescimento de nódulos de gipso em sedimentos carbonáticos ou argilosos
    - ex.: estrutura *chickenwire*
  - Pode ser encontrada em *sabkhas* ou águas profundas

Tipos de evaporito

- Anidrita nodular

Figure 7.1
Nodular anhydrite with an abundant calcareous (dolomicrite) matrix. Falces Formation (Oligocene), Ebro Basin, Spain. Photograph courtesy of Joseph M. Salvany, Universitat Politécnica de Catalunya, Barcelona.

Richi Lucchi (1996)

Boggs (2006)

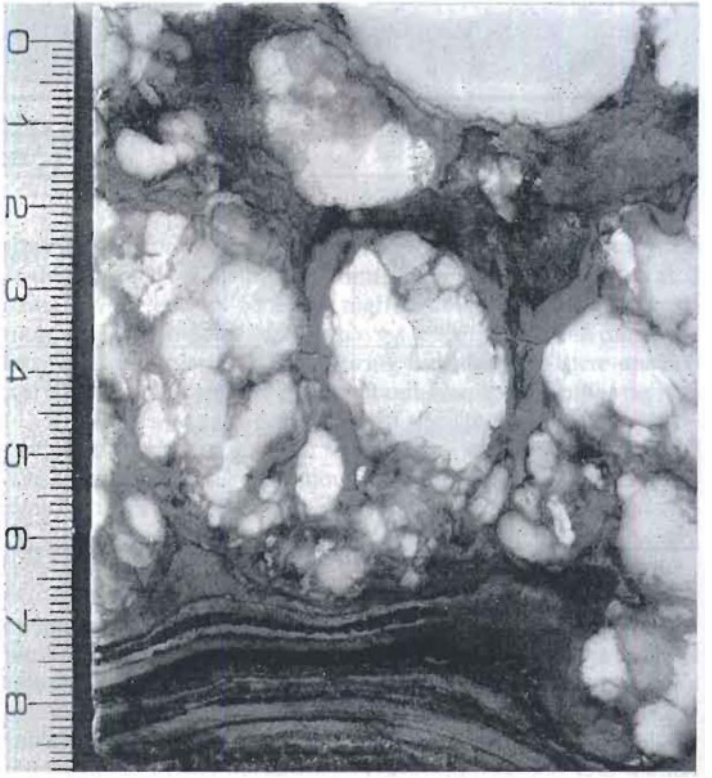

Tipos de evaporito

- Estrutura *chickenwire*

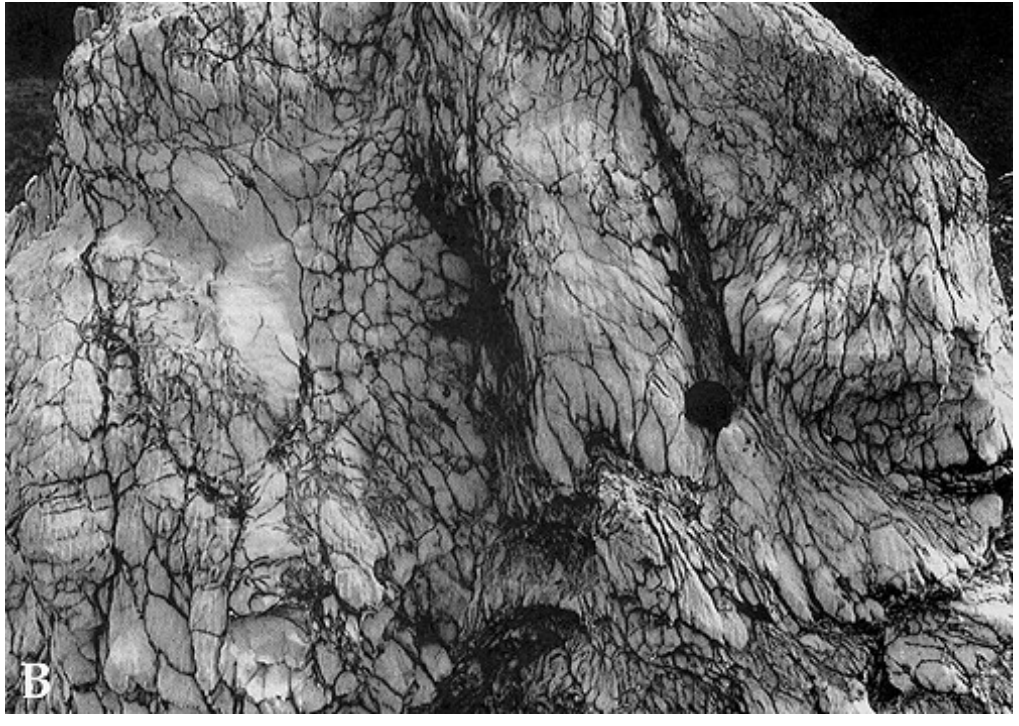

Richi Lucchi (1996)

◀ **11.13 Dolomitized evaporite unit showing chicken-wire structure. This represents calcareous clayey seams around original nodular sabkha gypsum. Lens cap 6cm.**
Cretaceous, near Benidorm, SE Spain.

Stow (2005)

Tipos de evaporito

- Anidrita laminada
  - Alternância de lâminas claras de gipso ou anidrita com lâminas escuras de dolomita e/ou mat. orgânica
    - Espessura milimétrica, lateralmente contínuas
  - Formadas (provavelmente) em águas calmas, abaixo da base do nível de ondas, águas rasas protegidas de agitação ou águas profundas

Tipos de evaporito

11.9 Thin gypsum beds (white-coloured) in lacustrine mudstone succession. Hammer 25cm.
Pliocene, Lake Eyre, Australia.

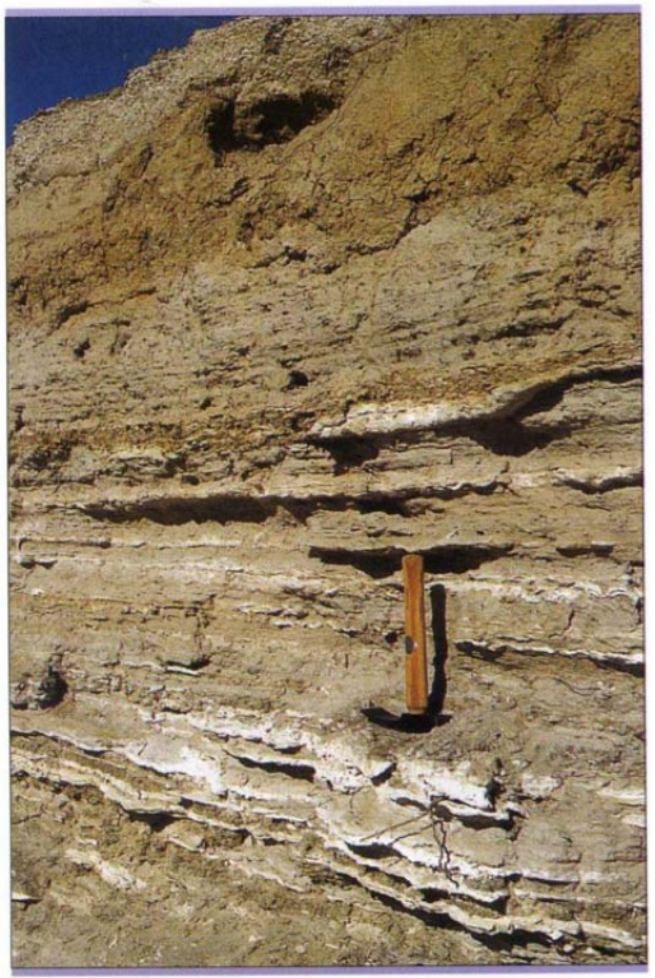

11.5 Finely laminated gypsum; note lenticular and micro-cross-lamination as clear evidence for current reworking of gypsum crystals; dark laminae slightly enriched in trace organics. Hammer 25cm.
Late Miocene, Psematisimenos, S Cyprus.

Stow (2005)

Tipos de evaporito

- Anidrita maciça
  - Coalescimento lateral de nódulos pode gerar uma camada espessa e irregular
    - Distorção provocada por crescimento pode resultar em estruturas enterolíticas
  - Anidrita maciça pode ser depositada também em condições uniformes de precipitação (presumivelmente)

Tipos de evaporito

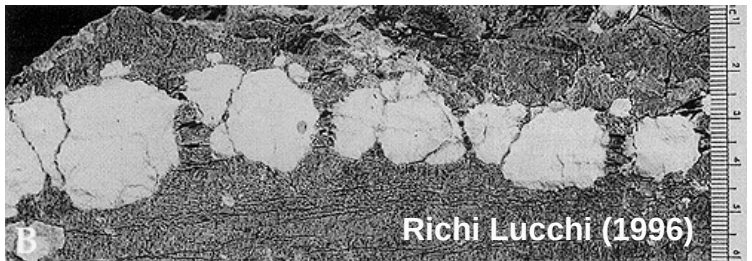

Early fabric of displacive enterolithic veins now preserved in late, secondary, (post-anhydrite) porphyrotopic gypsum. Soft Cockle Mb, Purbeck Formation, Worbarrow Tout . Ian West (c) 2005

https://wessexcoastgeology.soton.ac.uk/jpg-Worbarrow/5WB-entero-800.jpg

▶11.15 Detailed view of halite and polyhalite, nodular and crystalline with red and clear patches. Soft (scratches with fingernail) and with strong, salty taste. Width of view 10cm. *Triassic, Saskatchewan, Canada.*

Stow (2005)

Tipos de evaporito

- Halita
  - Pode ser formada como crostas, em águas rasas, ou depósitos laminados, em águas profundas
    - Espessura de depósitos pode superar os 1000 m
    - Geralmente associadas com lâminas de carbonato e anidrita

Tipos de evaporito

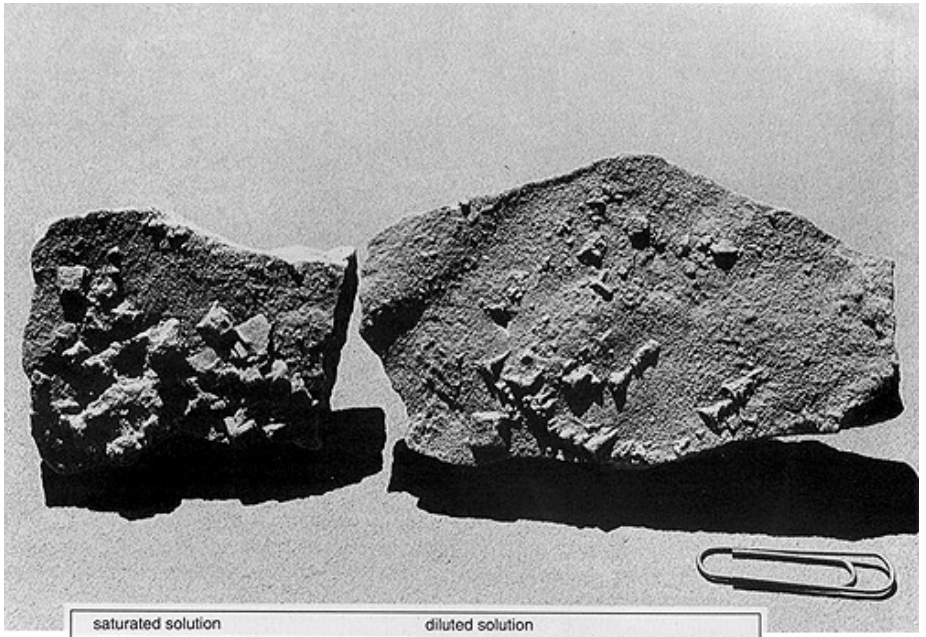

Richi Lucchi (1996)

Origem de Evaporitos

- Sequência de precipitação baseado em ensaios com água do mar
  - Evapora 50%$_{vol.}$ → formação de carbonatos
  - Evapora 80%$_{vol.}$ → precipitação de gipso
  - Evapora 90%$_{vol.}$ → precipitação de halita
    - Evaporação aumenta Mg/Ca, favorecendo dolomitização
  - Evapora >95%$_{vol.}$ → deposição de sais de Mg e K

Origem de Evaporitos

- Sequência de precipitação baseado em ensaios com água do mar

- Em depósitos naturais podem aparecer sequências parecidas, embora discrepantes
  - Em geral, $CaSO_4$ é muito mais frequente que sulfatos de Na e Mg em modelos teóricos

Estruturas

- Estruturas primárias
  - Estruturas cristalinas; decantação de cristais; nucleação de fundo
  - Podem ser transportados como partículas sedimentares → laminação cruzada, gradação inversa/normal, etc.
  - Muitos susceptíveis à deformação e alteração diagenética → frequentes nódulos e cristais pseudomorfos

Estruturas

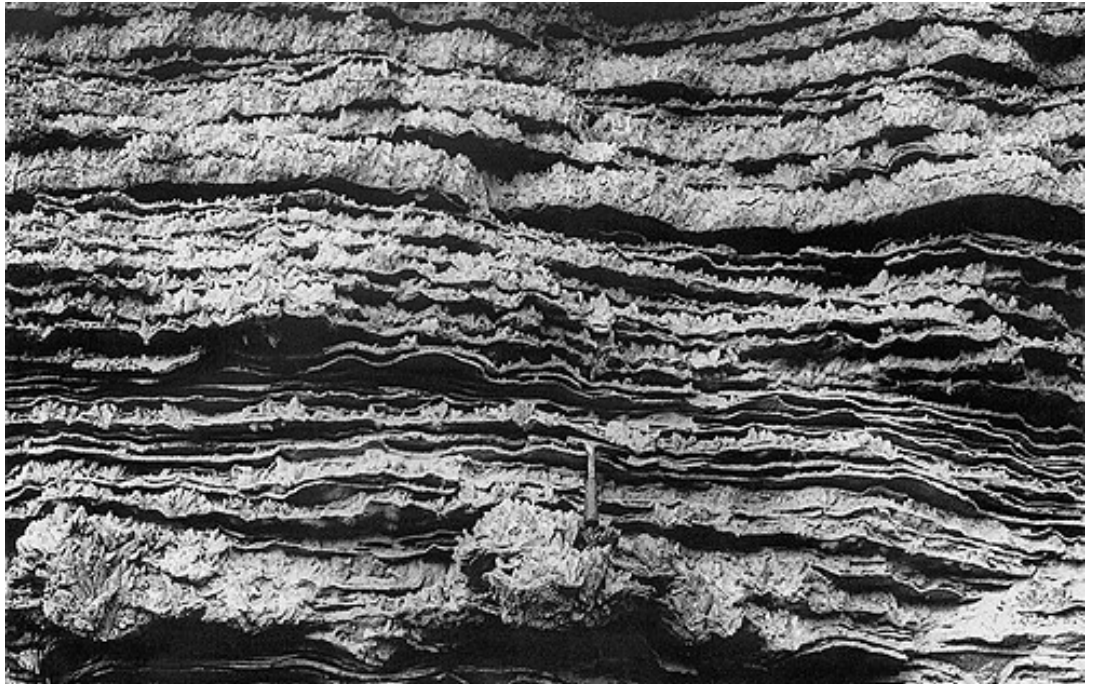

Richi Lucchi (1996)

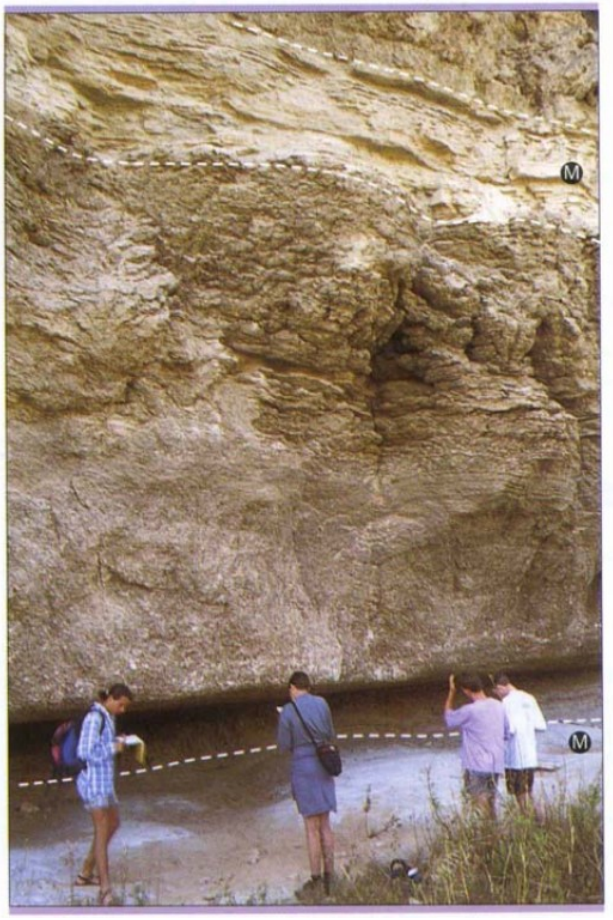

11.2 Thick gypsum unit (approx. 3.5m) sandwiched between micrite/marl intervals (M); note large cauliflower-like growth of gypsum in upper half of unit, and base of second gypsum unit visible near top; shallow-marine to lagoonal setting.
Late Miocene, Sorbas Basin, SE Spain.

Stow (2005)

Estruturas

11.7 Normally graded gypsum turbidite; note slight erosion at base, thin reverse-graded unit and highly fragmented gypsum clasts/grains.
Width of view 40cm.
Late Miocene, Pissouri Basin, S Cyprus.

11.6 Laminated and cross-laminated gypsum bed, indicating current reworking of gypsum crystals.
Hammer 25cm.
Late Miocene, Psematisimenos, S Cyprus.

Stow (2005)

Modelos deposicionais

- Evaporitos se formam em vários ambientes subaéreos e subaquosos rasos:
  - *Sabkhas* continentais e costeiros
  - Interdunas
  - Planícies salinas (*salt pans*)
- Exemplo moderno de ambiente de bacia profunda seria o Mar Morto
  - Contexto semelhante para os depósitos mais espessos e contínuos

Modelos deposicionais

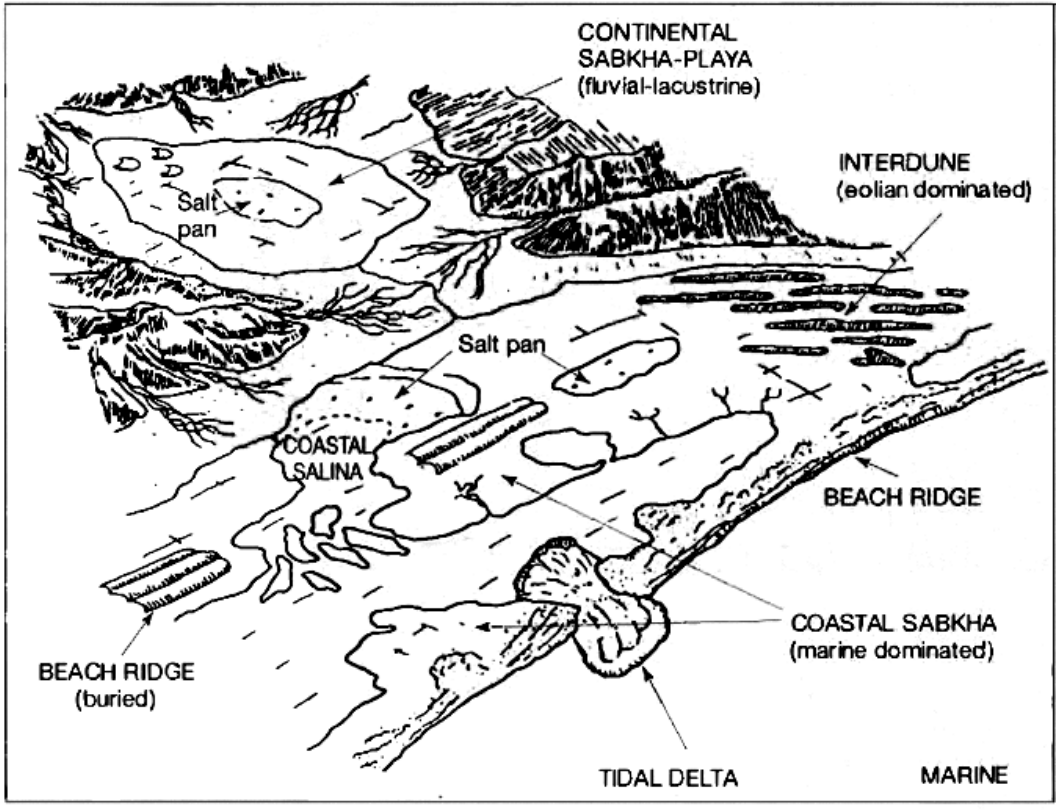

Figure 7.5
Principal settings in which modern evaporite deposits are accumulating. [From Kendall, A. C., 1984, Evaporites, in R. G. Walker (ed.), Facies models: Geoscience Canada Reprint Ser. 1, Fig. 1, p. 260, as modified slightly by Warren, 1989; reprinted by permission of Geological Association of Canada.]

Boggs (2006)

Modelos deposicionais

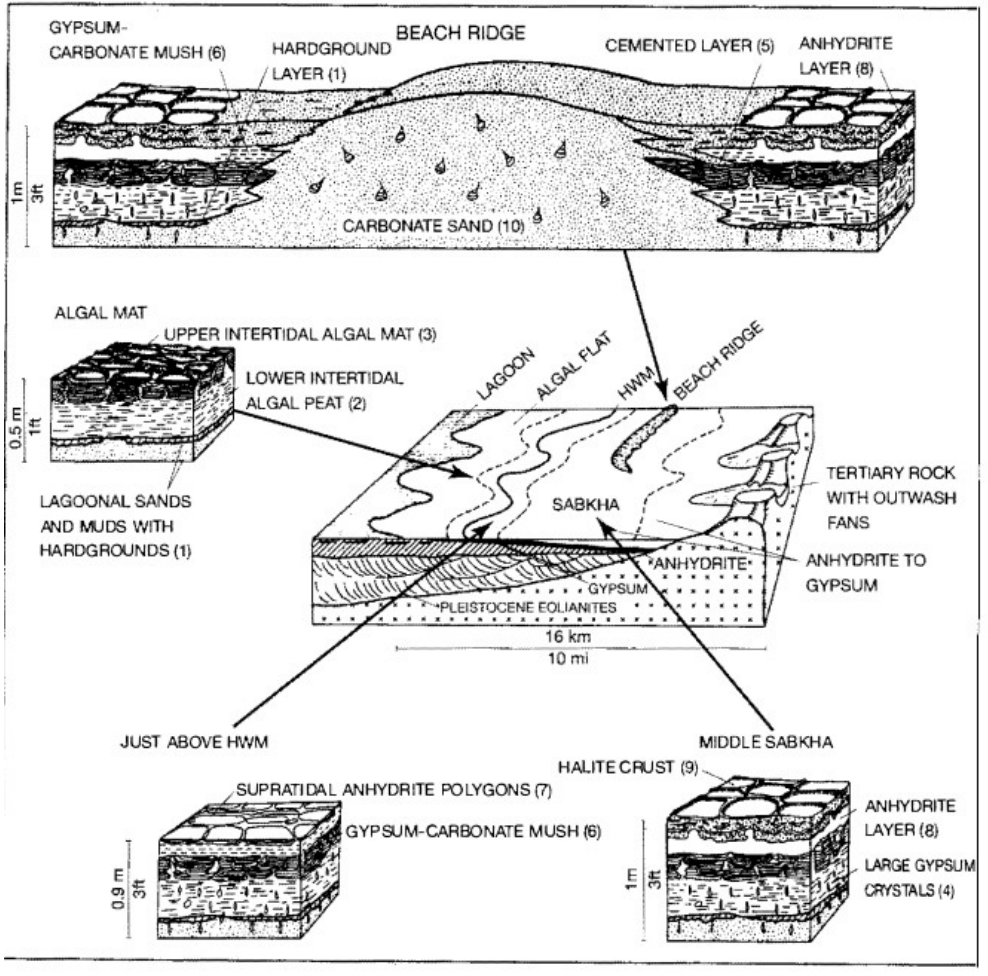

Figure 11.21
Schematic representation of vertical and lateral facies relationships in sabkhas of the Arabian Gulf. HWM = high-water mark. [From Warren, J. K., and G. St. C. Kendall, 1985, Comparison of sequences formed in marine sabkha (subaerial) and salina (subaqueous) settings—Modern and ancient: Am. Assoc. Petroleum Geologists Bull., v. 69, Fig. 2, p. 1015, reprinted by permission of AAPG, Tulsa, Okla.]

Boggs (2006)

Modelos deposicionais

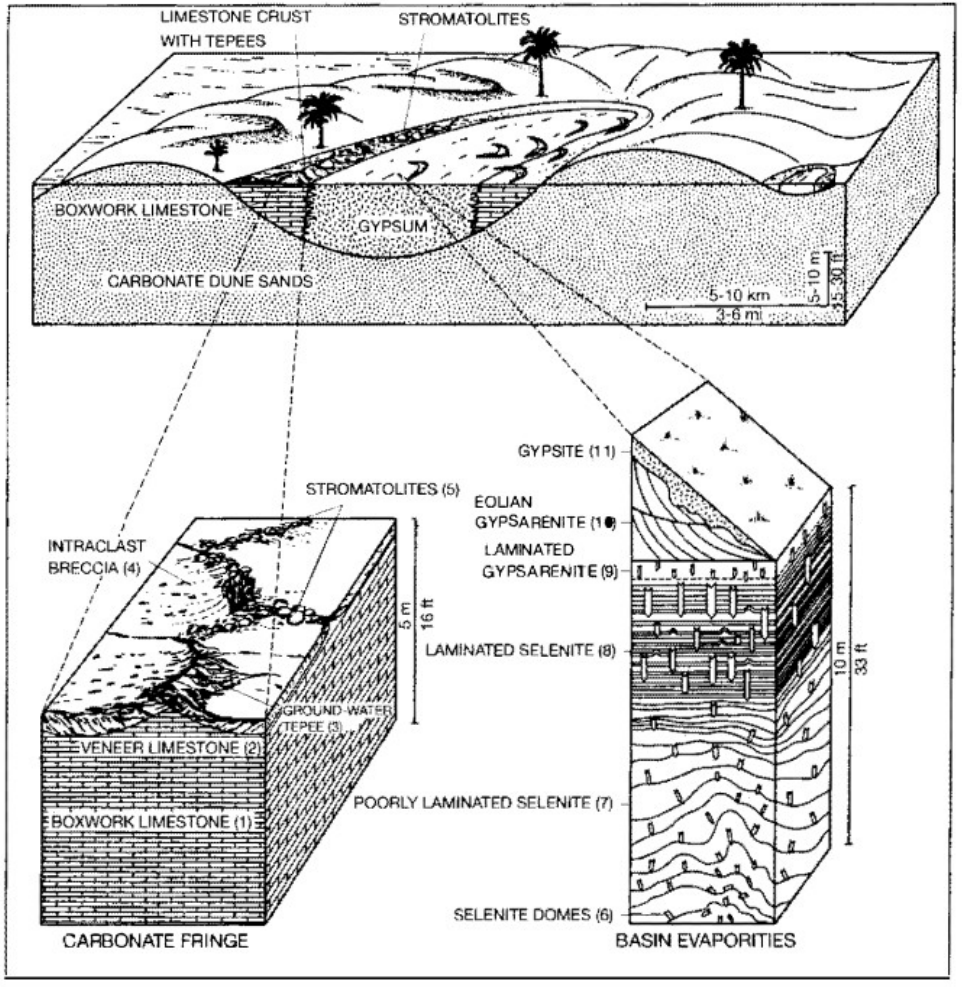

Figure 11.22
Environmental setting and typical evaporite facies in southern Australia salinas. [From Warren, J. K., and G. St. C. Kendall, 1985, Comparison of sequences formed in marine sabkha (subaerial) and salina (subaqueous) settings—Modern and ancient: Am. Assoc. Petroleum Geologists Bull., v. 69, Fig. 4, p. 1017, reprinted by permission of AAPG, Tulsa, Okla.]

Boggs (2006)

Modelos deposicionais

- Problemas:
  - No registro temos depósitos evaporíticos de mais de 1000 m de espessura
    - 1000 m de coluna de água evaporada resultaria em espessura de +/- 15 m de evaporitos
    - Se evaporar todo o Mediterrâneo teríamos ~60m de evaporitos

Modelos deposicionais

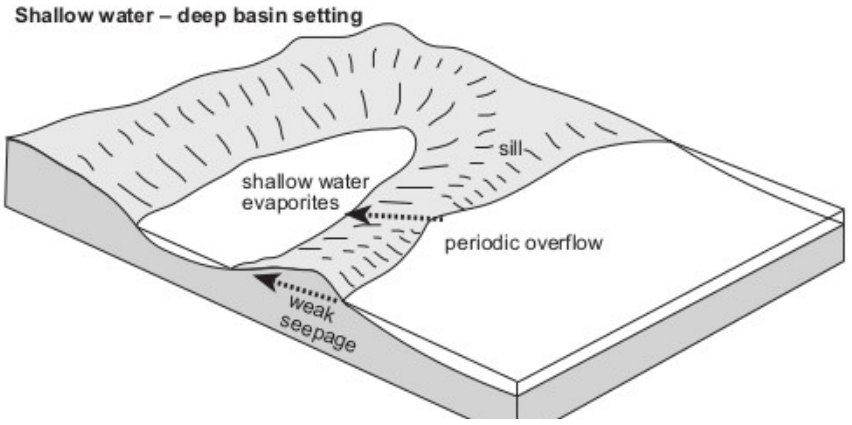

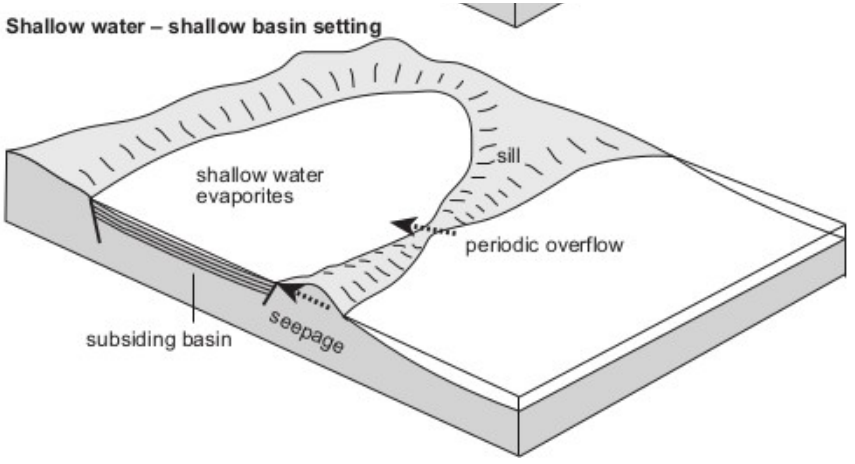

Fig. 15.19 Settings where barred basins can result in thick successions of evaporites.

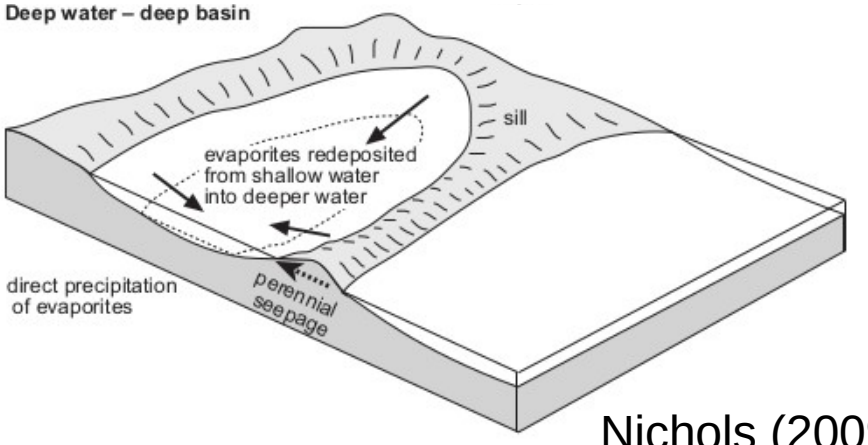

Nichols (2009)

Modelos deposicionais

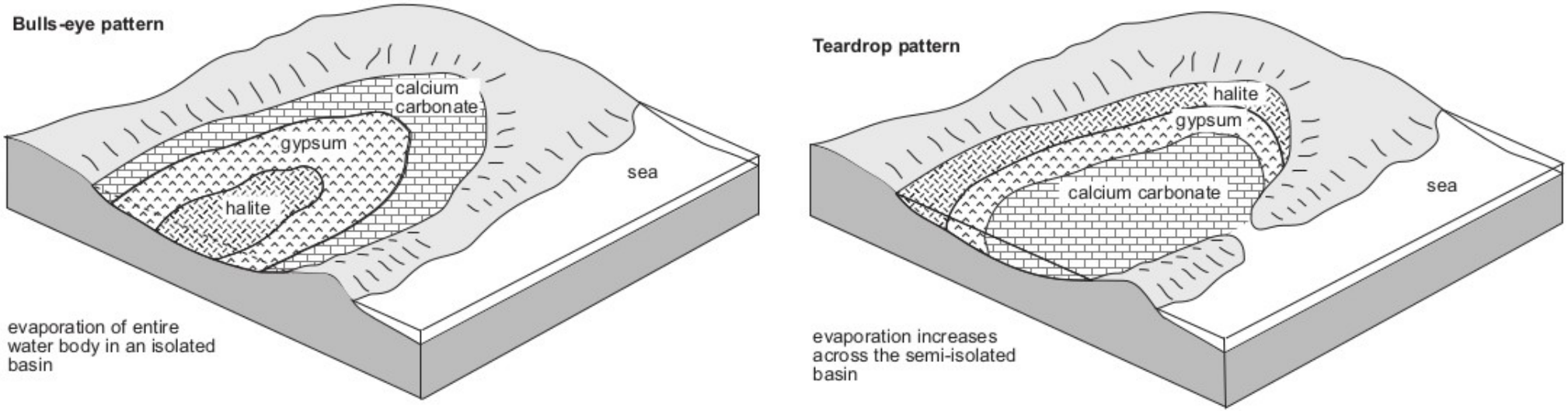

Fig. 15.20 (a) A barred basin, 'bulls-eye' pattern model of evaporite deposition; (b) a barred basin 'teardrop' pattern model of evaporite deposition.

Nichols (2009)

Gigante de sal do Atlântico Sul

Marine and Petroleum Geology 127 (2021) 104805

Contents lists available at ScienceDirect

Marine and Petroleum Geology

journal homepage: www.elsevier.com/locate/marpetgeo

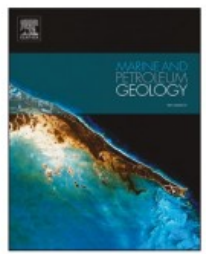

Research paper

Petrography, geochemistry and origin of South Atlantic evaporites: The Brazilian side

Peter Szatmari [a,*], Claudia Moré de Lima [b], Gabriella Fontaneta [b], Neilma de Melo Lima [b], Eveline Zambonato [b], Maria Rosilene Menezes [a], Juliana Bahniuk [b], Sirlene Lima Coelho [b], Milene Figueiredo [a], Claudio Pires Florencio [c], Rogério Gontijo [b]

Szatmari *et al.* (2021)

Gigante de sal do Atlântico Sul

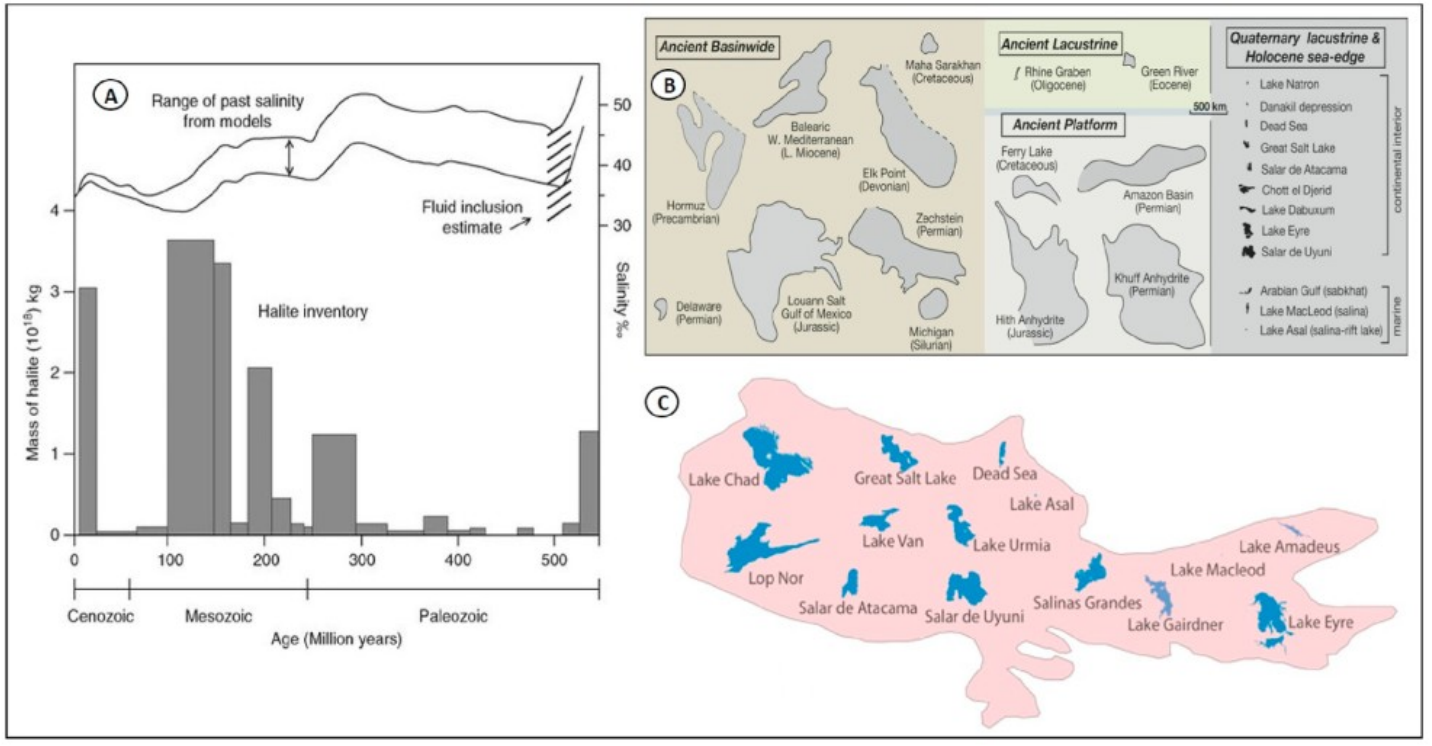

Fig. 1. Salt giants during the Phanerozoic. A) Above: Gradual decrease of the mean salinity of the ocean during the Phanerozoic, with periods of rising salinity between the deposition of salt giants. Below: Distribution and mass of existing halite deposits during the Phanerozoic. Modelling by Hay et al. (2006). Hay's two figures were joined by Knauth (2011). B) Giant salt basins compared to the modern evaporite depositing basins after James and Kendall (1992), modified by Warren (1999; 2016). C) The insignificant size of modern evaporite basins when placed within the Permian Zechstein Basin, shown in pink color (Warren, 2016). (For interpretation of the references to color in this figure legend, the reader is referred to the Web version of this article.)

Szatmari *et al.* (2020)

Gigante de sal do Atlântico Sul

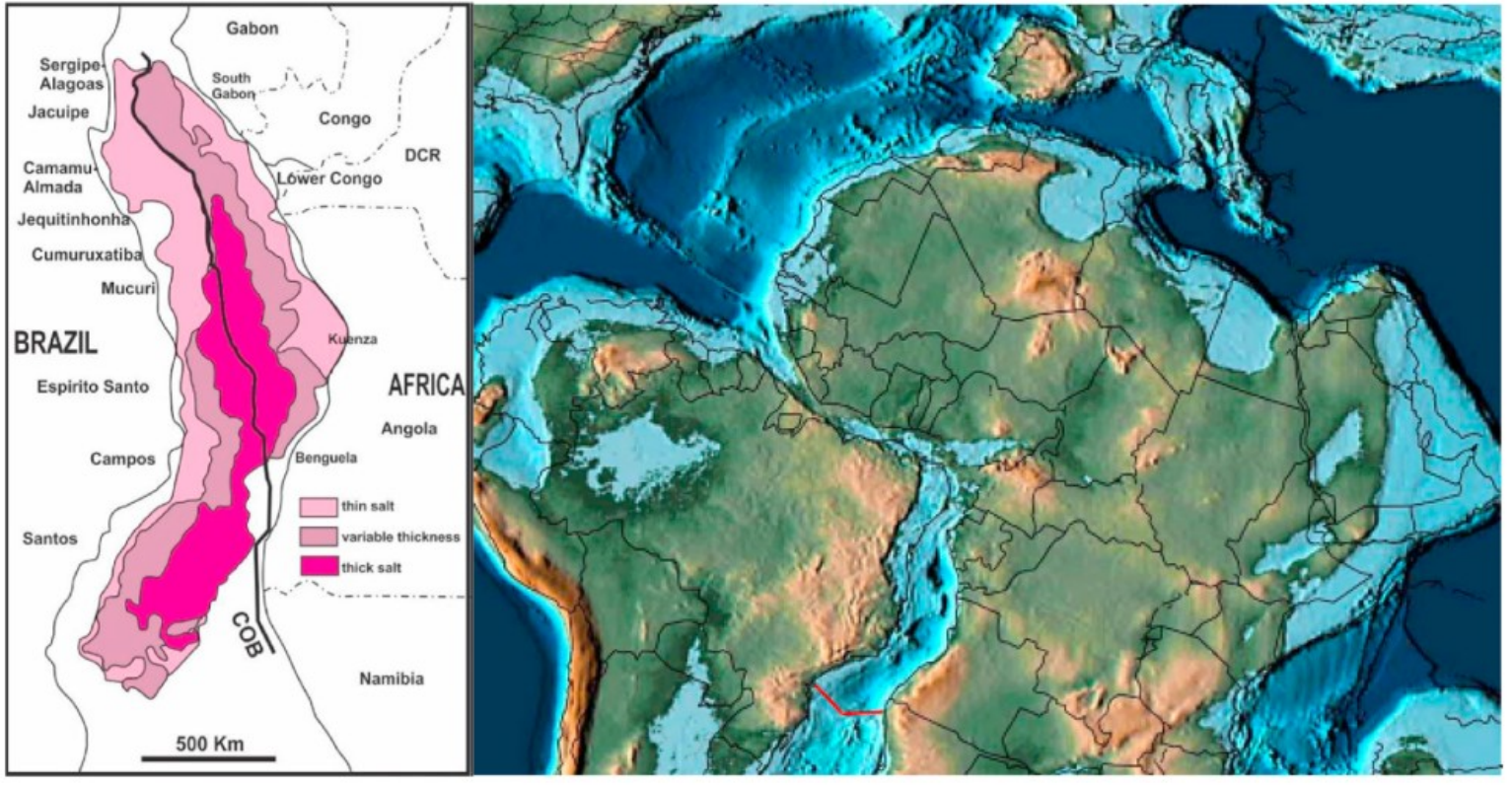

Fig. 3. The South Atlantic salt giant formed between the initial rift of the Equatorial Atlantic in the north and the proto-Rio Grande Rise – Walvis Ridge barrier in the south. Left: Present-day Aptian salt thickness of the South Atlantic (as modified by subsequent salt flow). After Lentini et al. (2010) modified by Rowan (2014). Right: Paleogeography of the South Atlantic when seawater ingression from the Central Atlantic Ocean through pull-apart equatorial rift basins permitted salt deposition. After Scotese (2016). Red line is added to show the proto-Rio Grande Rise – Walvis Ridge, the southern barrier of the salt basin forming over the Tristan plume (O'Connor and Duncan, 1990; Dingle, 1999; Arai 2014; Szatmari and Milani, 2016). (For interpretation of the references to color in this figure legend, the reader is

Szatmari *et al.* (2020)

Gigante de sal do Atlântico Sul

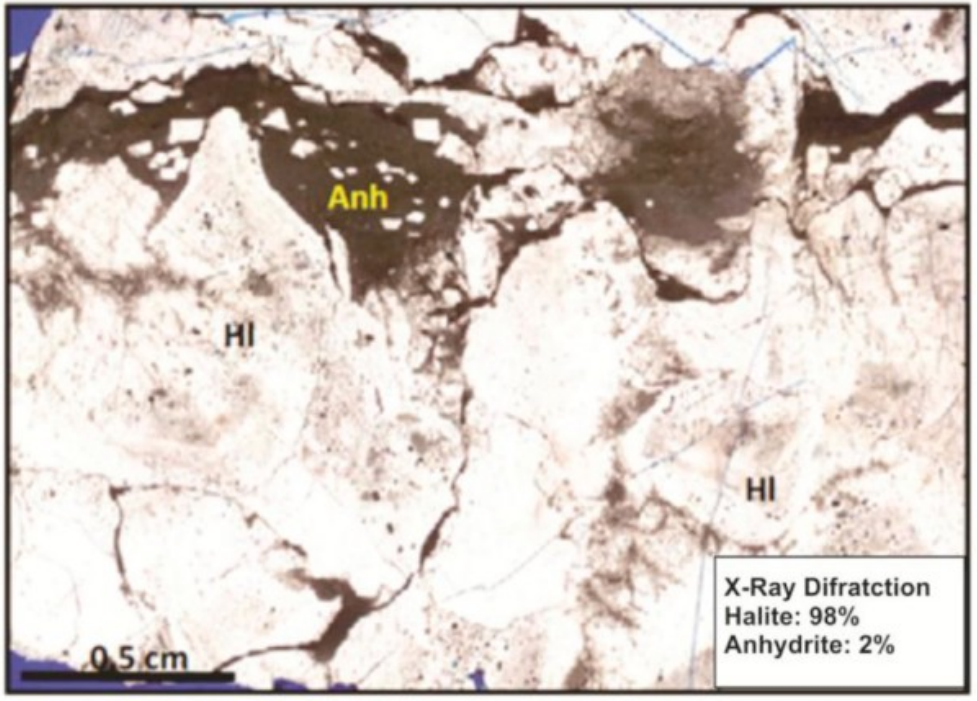

Fig. 8. Well 01, 1246.95 m, Cycle IV. Location in the core (arrow) and photomicrograph of coarse pyramidal chevron halite with anhydrite/gypsum lamina containing halite crystalloblasts. Part of the pyramidal crystals are zoned; zoning is marked by fluid inclusions and by frequent subhedral opaque 10 μm–50 μm crystals of undefined origin. At the top of the sample, subhorizontal stylolites are common. The anhydrite, in part replaced by gypsum, forms discontinuous beige laminae. Lamination is marked by films of organic matter. Halite crystalloblasts are common, dispersed in the fine anhydrite and oriented concordantly with the lamination.

Szatmari *et al.* (2020)

Gigante de sal do Atlântico Sul

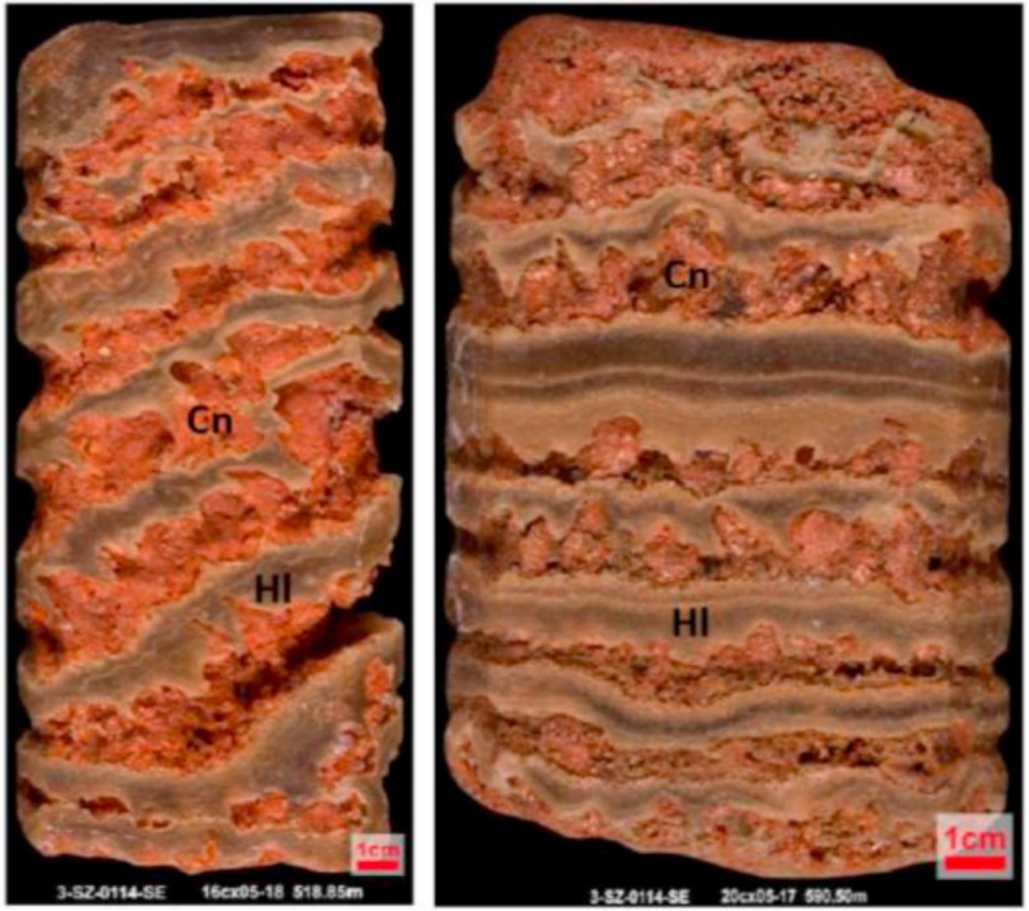

Fig. 10. Core samples composed of red prismatic carnallite intercalated with laminae and layers of fine halite (Muribeca Formation of the Sergipe Basin. Left: Well 02, 518.85 m, Cycle IV. Right: Well 02, 590.50 m, Cycle III. The carnallite is leached on the core surface by atmospheric water precipitated over the cores. (For interpretation of the references to color in

Szatmari *et al.* (2020)

Gigante de sal do Atlântico Sul

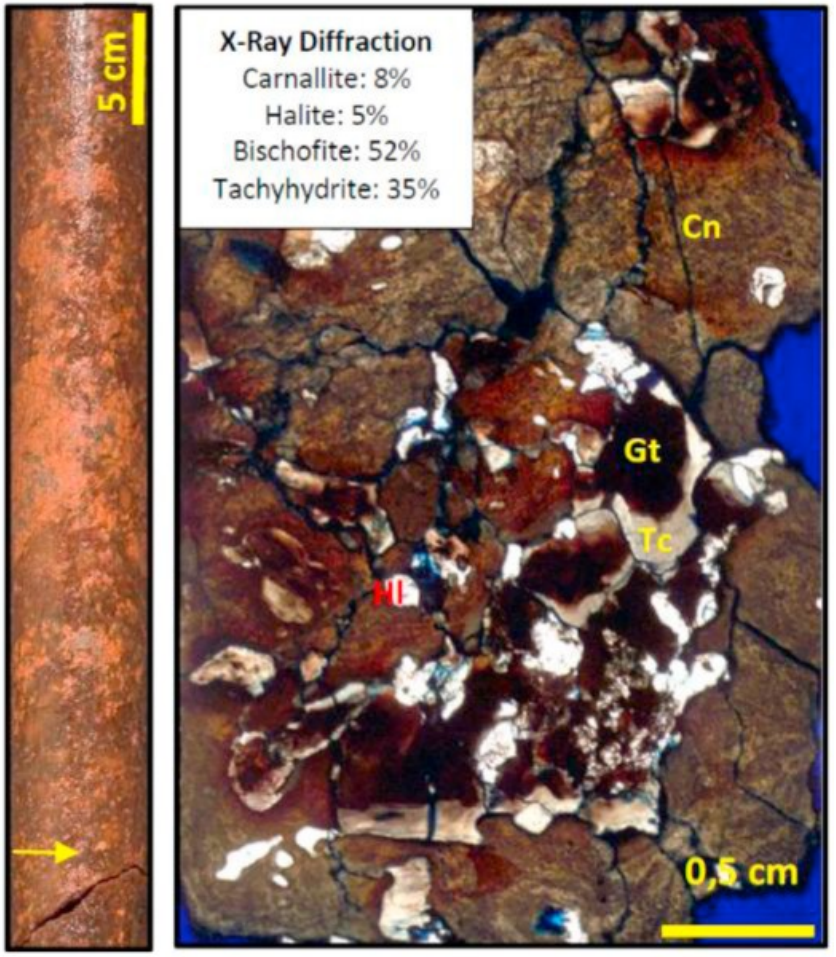

Fig. 16. Sample location in core (arrow) and photomicrograph of thin section of tachyhydrite, mosaic carnallite and halite. The carnallite forms a mosaic of anhedral brownish crystals. On the surface of the carnallite crystals, agglomerates of euhedral bischofite microcrystals are sometimes common. At the crystal contacts there are pores formed by decompression. Anhedral and subhedral tachyhydrite crystal inclusions are common, concentrated at the center of the sample. The cores of the tachyhydrite crystals are dark yellowish brown, perhaps owing to the presence of goethite. Halite occurs as dispersed fine amoeboid crystals and as inclusions principally in the tachyhydrite crystals (Well 01, 1195.10 m, Cycle V).

Szatmari *et al.* (2020)

Gigante de sal do Atlântico Sul

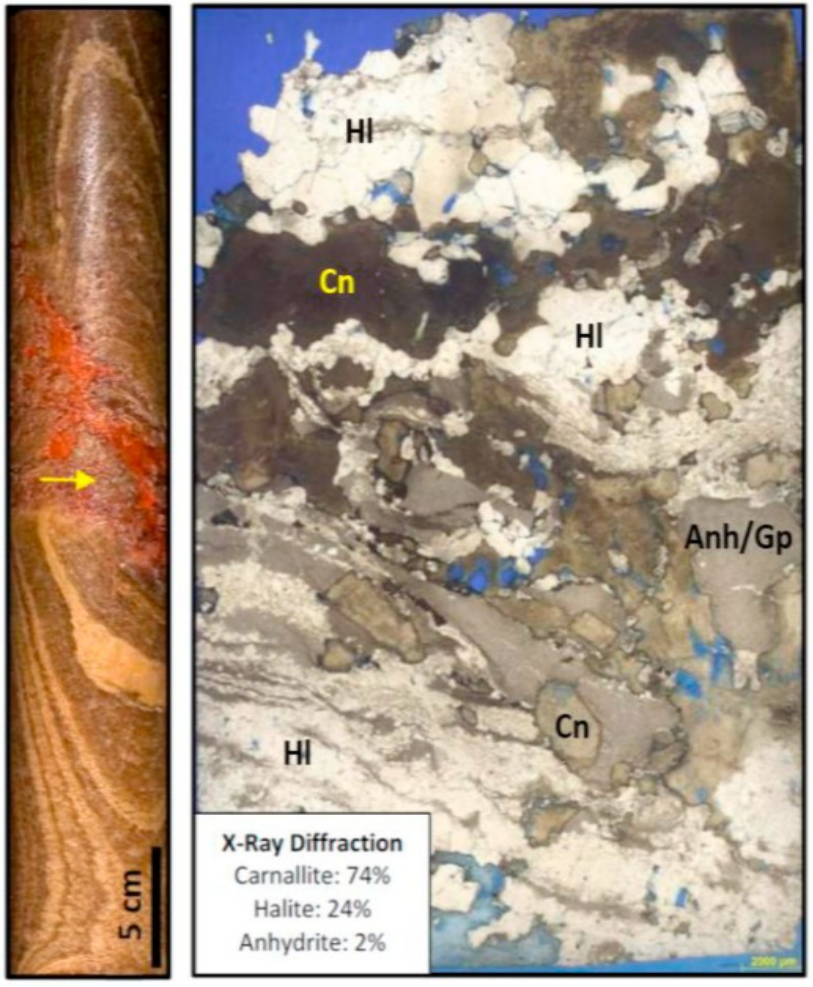

Fig. 11. Sample location in core (arrow) and photomicrograph of fine to medium crystalline mosaic hyaline halite, with network and laminae of very fine anhydrite/gypsum and medium to coarse, crystalloblastic to nodular reddish-brown carnallite. Extreme elongation (mylonitization) of the carnallite and halite crystals by salt flow, aided by the depth of the sample, is evident in both macroscopic and microscopic-optical examination (Well 01, 1102.40 m, Cycle VI). (For interpretation of the references to

Szatmari *et al.* (2020)

Gigante de sal do Atlântico Sul

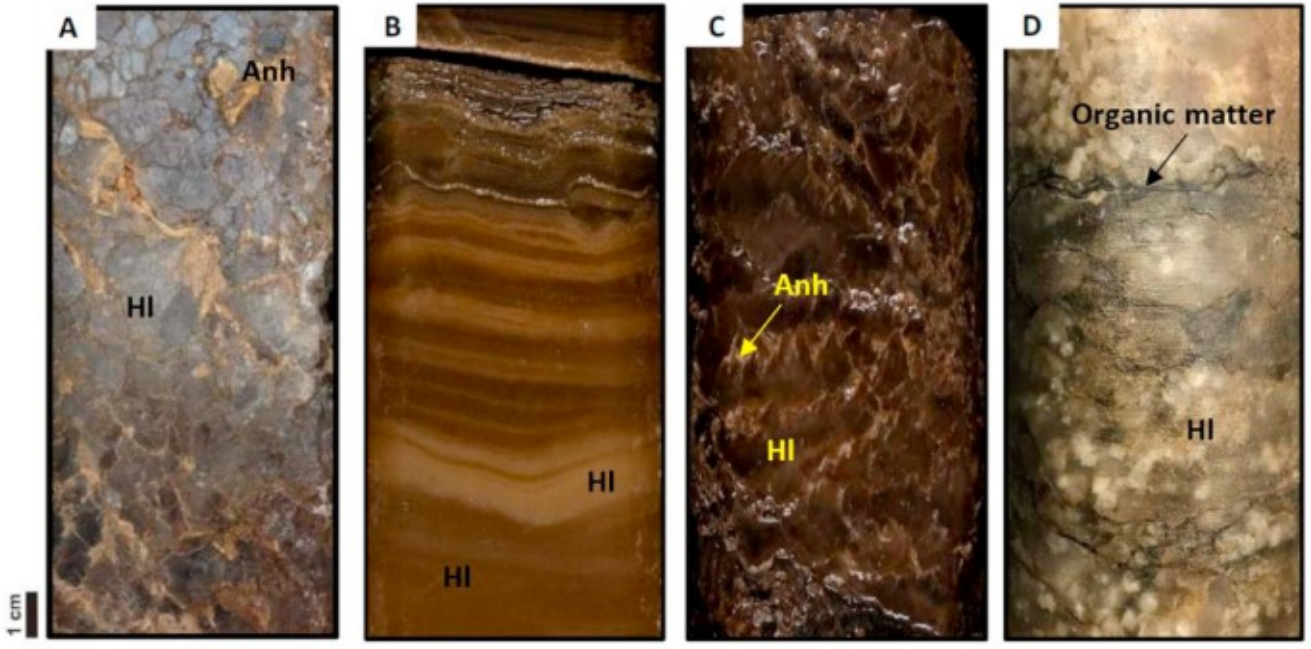

Fig. 23. Examples of halite facies observed in cores of the Muribeca Formation in the Sergipe Basin (Wells 02, 03 and 04). A) Well 02. Gray mosaic halite with fine anhydrite network possibly containing micrite. B) Well 03, 690.95 m, Cycle IX. Banded halite; banding is marked by varying amounts of fluid inclusions and organic matter. C) Well 03, 994.10 m, Cycle I. Prismatic halite with subparallel orientation. D) Well 02. Crystals of halite hoppers in mosaic halite. Note films of black organic matter.

Szatmari *et al.* (2020)

Gigante de sal do Atlântico Sul

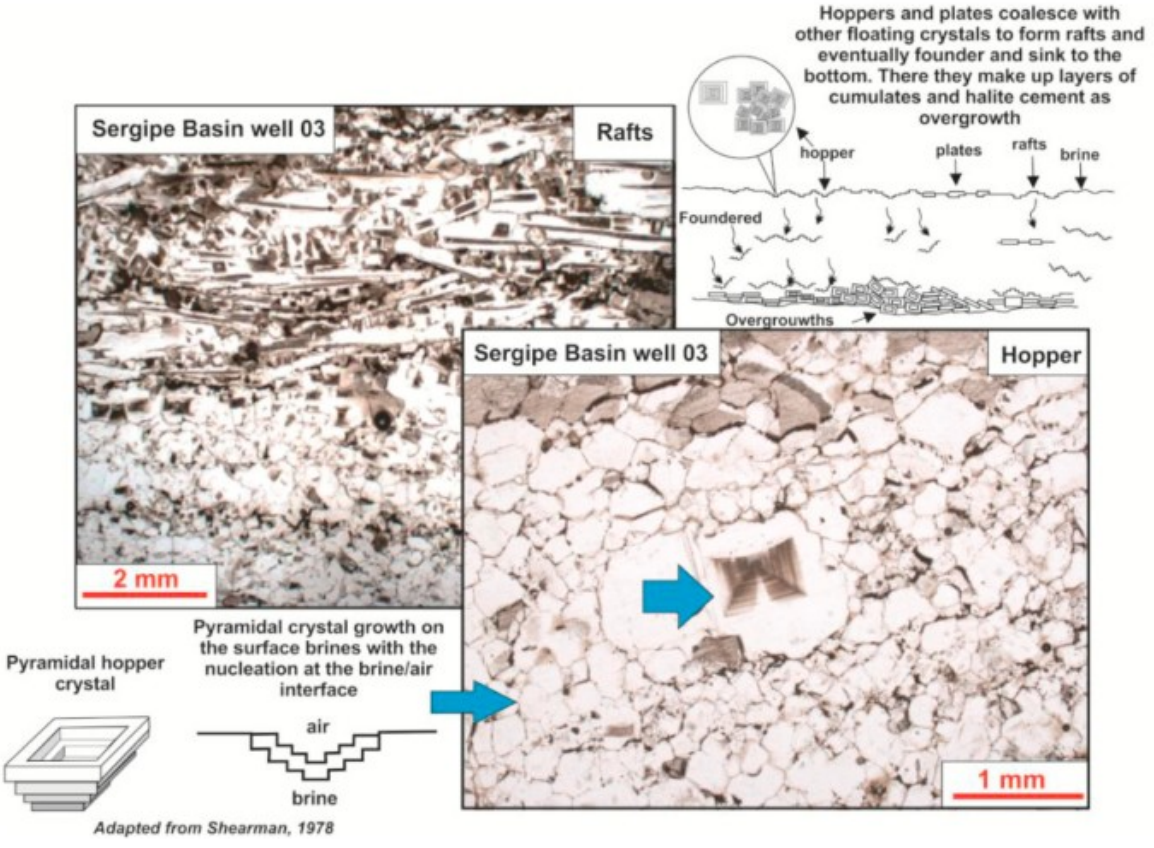

Szatmari *et al.* (2020)

Gigante de sal do Atlântico Sul

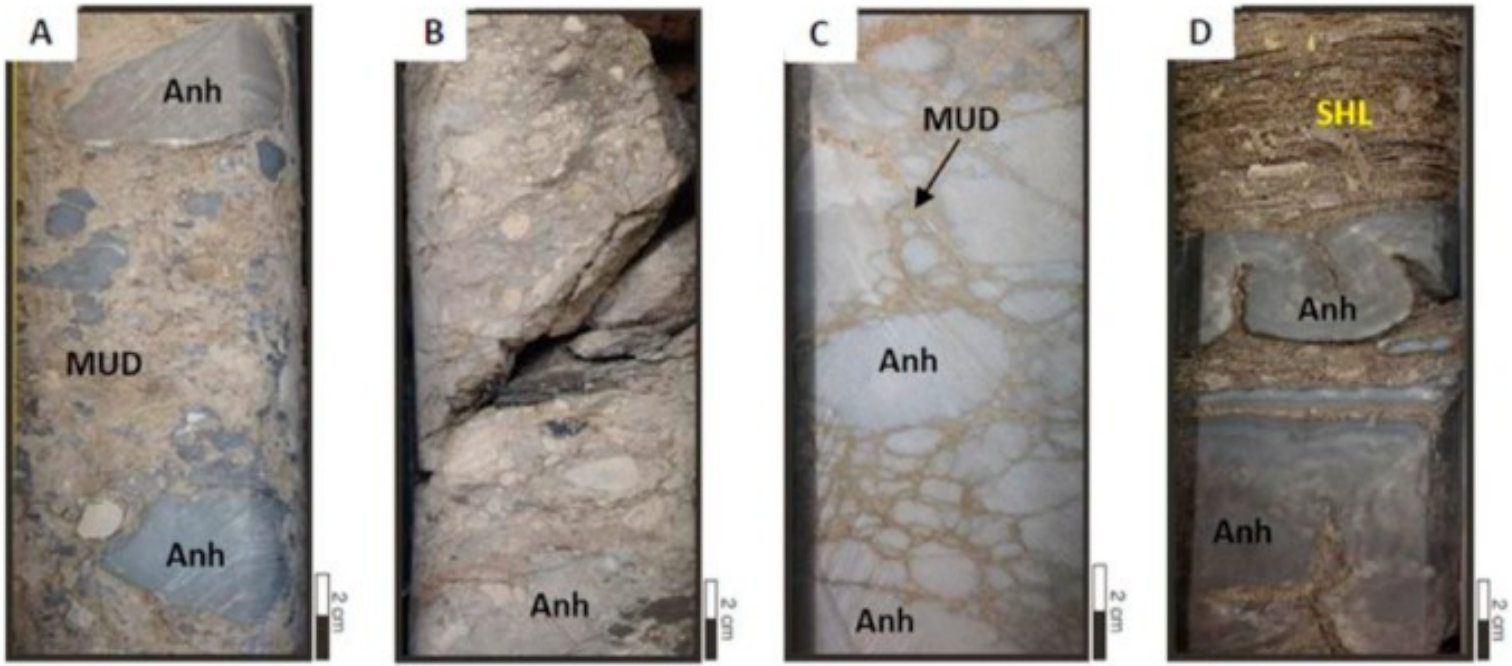

Fig. 25. Anhydrite breccia in the Muribeca Formation in the Sergipe Basin (Well 03, Cycle IX). A, B) Brecciated anhydrite in micritic matrix; C) Nodular anhydrite in micritic matrix; D) Enterolithic anhydrite in shale.

Szatmari *et al.* (2020)

Gigante de sal do Atlântico Sul

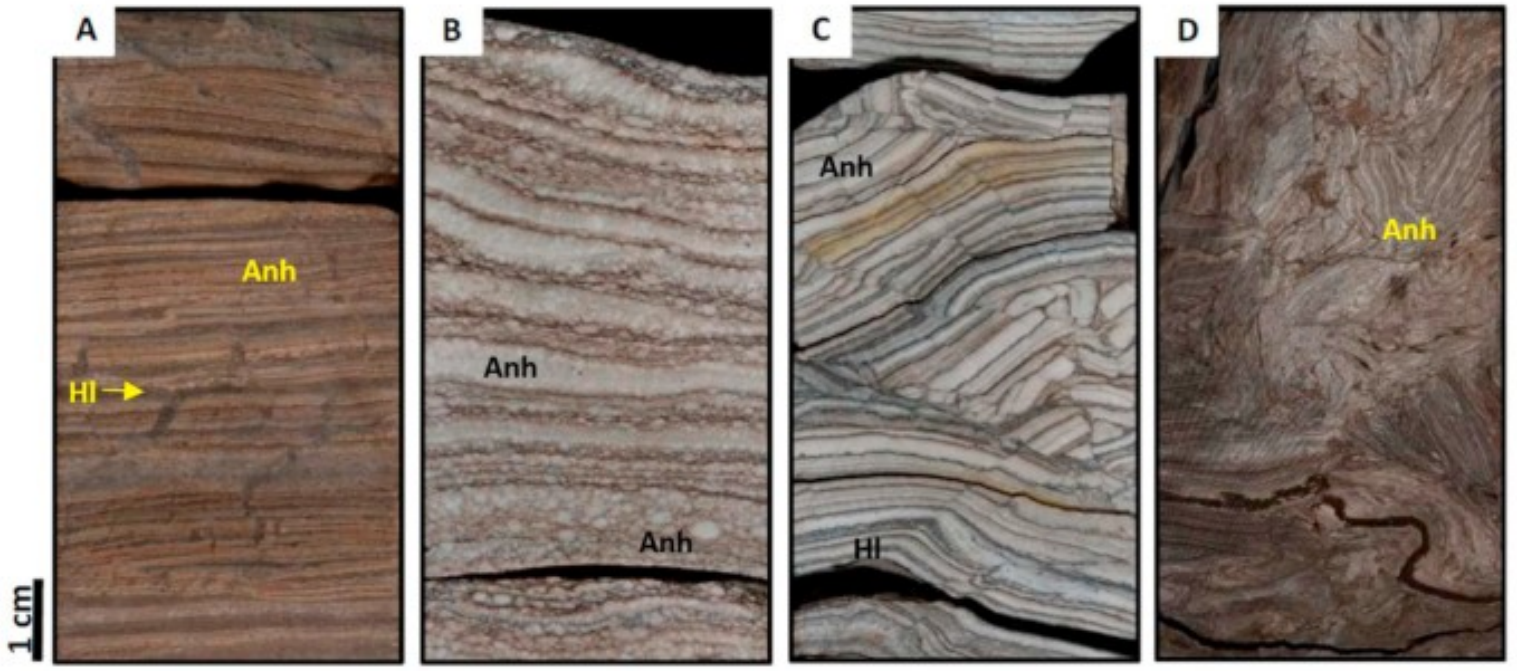

Fig. 27. Examples of anhydrite facies observed in cores of the Itaúnas Member of the Mariricu Formation, Espírito Santo Basin. A) Well 06, 1347.52 m. Interlamination of fine anhydrite and very fine halite with desiccation cracks. B) Well 08, 1123.20 m. Laminated prismatic anhydrite with small nodules largely restricted to individual laminae. C) Well 08, 1099.19 m and D) 1147.85 m. Laminated anhydrite collapsed and brecciated. D) 1147.85 m. Fine brecciated (and laminated) anhydrite.

Szatmari *et al.* (2020)

Gigante de sal do Atlântico Sul

Fig. 21. Collapse marked by a shale bed overlain by undisturbed halite interlaminated with anhydrite. Sergipe potash mine. After Vieira Mahado and Szatmari (2009).

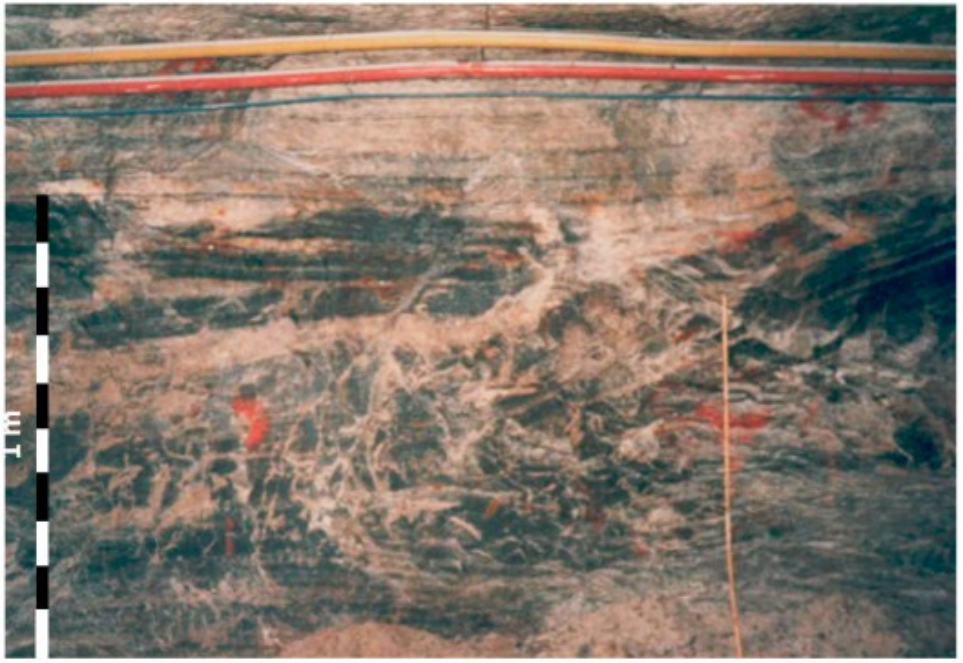

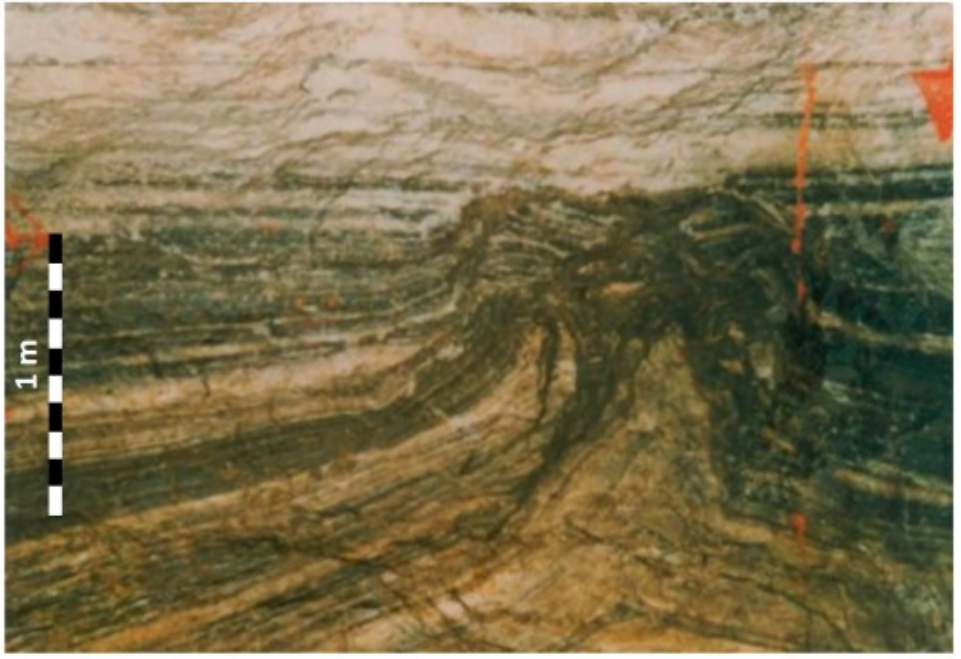

Fig. 22. Thrust fault in layered halite with dark shale bands removed along a horizontal unconformity surface overlain by undisturbed white halite. Sergipe potash mine. After Vieira Machado and Szatmari (2009).

Szatmari *et al.* (2020)

Considerações finais

- Evaporitos podem sofrer transporte de massa (*slumps* e correntes de turbidez), registrando gradação normal/inversa e até estruturas trativas
- Diagênese pode obliterar estruturas por mudanças de volume e deformação interna
- Soterramento e tectonismo também podem destruir estruturas sedimentares
  - Diapirismo pode criar diápiros com quilômetros de soerguimento (ex.: evaporitos das Bacias da Margem Atlântica
- Importância econômica: sais de aplicação industrial (e.g. trona) e de aplicação na agricultura (ex.: K para fertilizantes)

Referências

Boggs S. 2006. Principles of sedimentology and stratigraphy. 4th Ed. Prentice Hall. 662p.

Nichols, G. 2009. Sedimentology and stratigraphy. 2nd Ed. Willey-Blackwell. 419p.

Ricci Lucchi, F. 1996. Sedimentographica: photographic atlas of sedimentary structures. Columbia University Press On-Line. www.columbia.edu/dlc/cup/ricci/index.html

Stow, D.A.V. 2005. Sedimentary rocks in the field: a colour guide. CRC Press. 320p.

Szatmari, P. et al. 2021. Petrography, Geochemistry and Origin of South Atlantic Evaporites: The Brazilian Side. Marine and Petroleum Geology, 127: 104805.